Proceedings of the 25th Annual International Conference of the IEEE EMBS
Cancun, Mexico • September 17-21, 2003

MRI Systems as a Mean of Propulsion for a Microdevice in Blood Vessels

J-B. Mathieu[1], S. Martel[1], L'H. Yahia[2], G. Soulez[3], G. Beaudoin[3]
[1]Department of Computer Engineering, NanoRobotics Laboratory, École Polytechnique de Montréal, PQ, Canada
[2]Department of Mechanical Engineering, Biomechanics/Biomaterials Research Group, École Polytechnique de Montréal, PQ, Canada
[3]Radiology Department, Faculty of Medicine, Université de Montréal, PQ, Canada

Abstract—**The use of an MRI system as a mean of propulsion for a small robot for applications in blood vessels is being studied. The strong and variable magnetic field of the MRI system will exert three dimensional propulsion force to a ferromagnetic core that will be embedded onto the future small robot. The paper describes studies conducted concerning the ability of MRI gradients to propel a ferromagnetic body and the possibility to use MR images to track it. Experimental studies showed that a 3.175 mm diameter, 1010/1020 carbon steel sphere was able to withstand a maximum flow of 0.4115 l/min. in a 6.35 mm diameter tube when a magnetic field gradient of 18 mT/m was applied on it. Images made with spin echo and gradient echo sequences showed that imaging distortions (artifacts) caused by ferromagnetic cores are several times larger than the size of the core itself. It is critical to measure accurately the position of the future robot. The elimination or reduction of such ferromagnetic artifacts is currently a serious problem. Therefore, alternative solutions to the imaging problems like artifact cancellation, artifact pattern tracking softwares or magnetic tracking systems need to be developed.**

Keywords—**Magnetic resonance imaging, microrobot, blood vessels, magnetic propulsion, ferromagnetic artifacts**

I. Introduction

The project's long-term goal is to provide surgeons with a microdevice capable of being controlled inside medium and small blood vessels. Some Medical applications of such a microdevice are Minimally Invasive Surgeries (MIS) like angioplasties, biopsies or highly localized drug deliveries for chemotherapy. The smaller these devices are, the wider their operating range becomes through accesses to the finest blood vessels such as capillaries. Magnetic Resonance Imaging (MRI) systems provide adequate magnetic field and gradients for propulsion and are already present in almost every hospital. Therefore, they were chosen as the magnetic field and gradients generator for the future microrobot that is referred to as MR-Sub: Magnetic Resonance Submarine. MR-Sub will be released by catheter and will be externally guided using a control software able to track it, compute its trajectory and then determine the MRI gradients to be applied on it.

Magnetic control is extremely promising for miniaturized systems targeted at in vivo applications. Micromotors are the other propulsion systems that could be envisioned for such applications. Nevertheless, they have the drawback of requiring precise and complex assemblies of several moving parts, which increase chances of failure and make miniaturization more difficult. They need to include an energy source or an energy conversion device, a device to convert torque into motion force (propeller, flagella...) and a way to control the direction of the driving force. The smallest ultrasonic motors existing have a 1.4 mm diameter and are 5.0 mm long [1]. The size of the propulsion system alone is already too big for vascular applications. We believe that the easiest and most effective way to design a propulsion system is to rely on an external magnetic field to move ferromagnetic particles. Magnetic propulsion researches for minimally invasive surgery have been performed at University of Virginia [2] and at Tohoku University [3]. Our goal is to control the future robot with magnetic field gradients inside the blood vessels. The blood flows and the diameters of the blood vessels that are targeted determine the drag force encompassed by the microdevice. These parameter are linked to the medical application that has to be performed and determine the quantity of ferromagnetic particles needed, which is related to the size of the microdevice. A ferromagnetic propulsion core is easy to fabricate and to miniaturize as the force is directly proportional to the ferromagnetic volume, and all the energy needed comes from outside. There is no need for a propeller or propulsion device of any kind and changing the direction of the magnetic field gradient $\nabla\vec{B}$ vector allows steering of the system.

This paper describes the results of our preliminary MRI control tests and magnetic resonance imaging tests. Their goal was to validate theoretical calculations by experimentations where magnetic and drag forces were confronted, and to evaluate the imaging distortions induced by the presence of ferromagnetic materials in an MRI system.

II. Background

Because of its larger diameter, the arterial system is being considered as the initial target location where the microrobot will be implanted. Later, with further miniaturization and more precise imaging techniques, smaller regions such as capillaries will also be considered. The dimensions of the blood vessels in human typically range from 25 mm in diameter (aorta) to approximately 8 μm (capillaries) [4]. The blood flow in the arterial system is pulsatile and much faster at the exit of the heart (ascending aorta: maximal systolic

This work is supported in part by the Canada Research Chair (CRC) in Conception, Fabrication, and Validation of Micro/Nanosystems and by the Natural Sciences and Engineering Research Council of Canada (NSERC).

velocity is 1120 mm/s) [5]. The blood velocity decreases away from the heart to a couple of cm/s then mm/s[4].

The torque and the force created by an MRI system can be calculated from [6]

$$\vec{\tau}=\vec{m}\times\vec{B}=\vec{M}*V_{ferro}\times\vec{B} \quad (1)$$

$$\vec{F}_{\text{magnetic}}=\vec{M}.V_{ferro}\nabla\vec{B} \quad (2)$$

In (1) and (2), τ is the magnetic torque (N.m), $\vec{F}_{\text{magnetic}}$ is the magnetic force (N), $\vec{M}$ is the magnetization of the material (A/m), V_{ferro} is the volume of the ferromagnetic body (m^3), $\vec{B}$ is the magnetic induction (T) and $\nabla\vec{B}$ is the gradient (spatial variation) of the magnetic induction (T/m).

The drag force of a rigid sphere in a rigid cylindrical tube is a function of the density of the fluid (ρ), relative velocity of the sphere to the fluid (V), frontal area (A), drag coefficient of the sphere (C_D), Reynolds number (Re) and ratio of sphere diameter to cylinder diameter (λ) [7].

If the magnetic force created by the MRI system is stronger than the drag force of the blood flow on the microrobot, control in displacement will be possible.

III. Materials and Methods

The goal of the first experiment (sample 1) was to match the magnetic and drag force acting on a ferromagnetic sphere in a cylindrical tube using an MRI system. The goal of the second experiment (sample 2) was to observe the effect of ferromagnetic bodies on the images created by an MRI system. A description of the ferromagnetic samples used for the experiments can be found in Table 1. These properties were measured with a 155 Princeton Applied Research Corporation (PAR) vibrating sample magnetometer and 610 Hall effect Bell Gaussmeter. All MRI tests were performed on a 1.5-T Siemens Magnetom Vision system that fully magnetizes the samples ($\vec{B}_{sat}$).

A. Experiment 1: MRI Propulsion

A turbine pump was placed outside of the MRI room to create a flow through a straight graduated PMMA tube located inside the MRI bore (6.35 mm diameter, 1800 mm long). The carbon steel ball was placed in the straight tube. The velocity profile of the fluid is fully developed when it reaches the sphere.

TABLE I
FERROMAGNETIC SAMPLES TESTED

Sample number	Description	B_{sat} (T)	Magnetizing induction (T)
1	1010/1020 Carbon Steel Ball, 3.175mm. Dia., Grade 1000	1.67	0.717
2	440-C Stainless Steel Precision Ball, 1.588 mm. Dia., Grade 24	1.14	0.733

The flow was measured and regulated with a variable-area flowmeter with control valve. Fig. 1. and 2 illustrate the set-up. A y, z, magnetic field gradient of 18 mT/m was applied with a cycle of 10ms on and 2 ms off. As the magnetic torque generated by the intense magnetic field (1.5T) is more than 52000 times stronger than the torques created by all the other forces, the sphere cannot roll inside the tube [8]. Friction between the sphere and tube walls are not considered in this study as MRI systems providing gradients strong enough to levitate the robot will be used in the future. Moreover, this important force of friction can be used as an anchoring system. The y part of the gradient aimed at reducing the static and dynamic friction force between the ball and the PMMA tube.

An 18mT/m gradient is not strong enough to levitate the sphere. Therefore, mechanical impulse was applied on the PMMA tube in order to detach the ball from its walls. To take the measurements, the gradients were turned on while the valve of the flowmeter was opened completely allowing maximum flow in the PMMA tube. Then, the valve of the flowmeter was progressively closed until the ball starts moving against the flow. Finally it was adjusted until an equilibrium state of the ball is reached. The measurements were repeated with a 6mT/m horizontal gradient and 18mT/m vertical gradient. The results of the equilibrium flow are recorded in Table 2.

B. Experiment 2: Evaluation of Ferromagnetic Artifacts

In order to be able to measure an MRI signal, ferromagnetic bodies have to be immersed in an aqueous medium. Oranges contain water and their well-known structure allows easy recognition of signal and geometric artifacts. As such, the ferromagnetic sample was placed inside a small orange with approximately 50 mm in diameter.

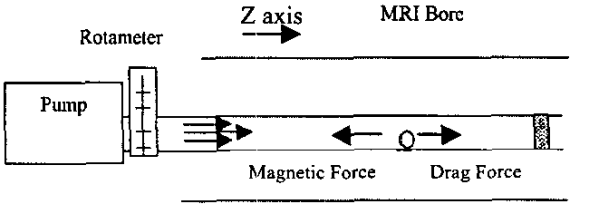

Fig. 1. MRI propulsion set-up for experiment 1

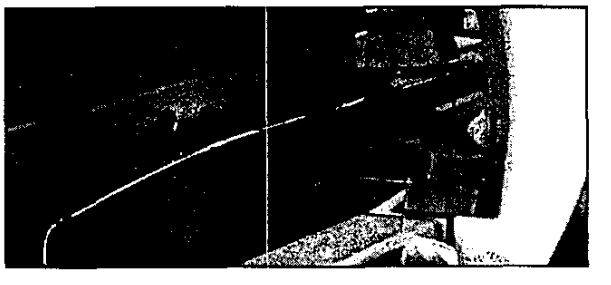

Fig. 2. MRI bore equipped with MRI propulsion set-up

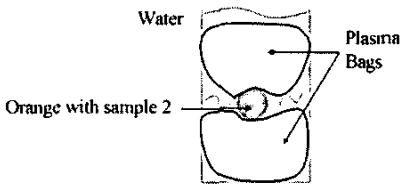

Fig. 3. MRI Set-up for experiment 2

The orange was immersed inside of a water tank. It was placed between two plasma bags full of water that prevented it from moving while imaging. This set-up (Fig. 3.) offered a view of one single artifact and an aqueous volume large enough to contain it completely. The shim routine was able to converge. Fast gradient echo scans of the imaging volume were used for the localization of the ferromagnetic body (imaging series A shown in Fig. 4). The imaging series B was done using spin echo sequences with a 3 mm slice thickness and a 3 mm distance between slices. Series B was made in the sagittal plane and phase encoding was head-feet (Fig. 5.).

IV. Results

Peripheral arteries have diameter and flow of the same order of magnitude as the diameter and flow that were used in the experiment 1. As shown by results in Table 2, it is possible to use a standard MRI system to move a ferromagnetic sphere inside a duct with Reynolds number close to real arteries (fluid density and viscosity, flow, diameter).

Ferromagnetic bodies imaging results are the following. As shown in Fig. 4, the effect of ferromagnetic presence on gradient echo images are geometric distortions as well as signal losses. Spin echo sequences are less sensitive to magnetic field distortions caused by ferromagnetic bodies [9]. However, the images acquired using a spin echo sequence are longer to generate (Fig. 5).

TABLE II
FLOW AND MEAN VELOCITY MEASUREMENTS

Magnetic field Gradient (mT/m)	Flow (l/min.)	Mean Velocity (m/s)
18	0.4115	0.217
6	0.1775	0.093

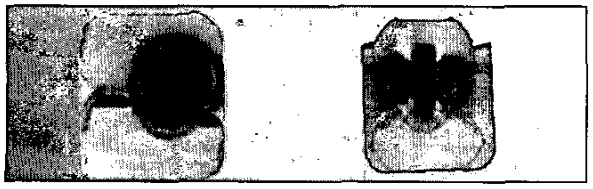

Fig. 4. Imaging series A

Serious geometrical distortions as well as zones with low signal or saturated signal were observed. The volume of the artifacts that were generated was larger than we first predicted. This size problem makes the localization of a ferromagnetic body in the image more difficult.

V. Discussion

The fluid used in experiment 1 was water instead of blood. The density of the Blood is 1.05 times higher than the density of the water at the same temperature and its behaviour is Newtonian at this tube diameter [5]. As drag forces are proportional to the density of the fluid it will be 1.05 times stronger in blood.

If the immersed body had been streamlined instead of spherical, its drag coefficient would have been lower and it would have been able to withstand a higher flow [10].

If the tests had been made with a smaller sphere compared to the tube, the maximum flow would have been comparatively higher [7].

The samples used in these tests were 1010/1020 carbon steel with a saturation induction B_{sat} of 1.67 T. It is reported in the literature that the CoFe alloys provide the highest saturation induction (B_{sat} = 2.45 T for permendur) [11]. Using a ferromagnetic material with a stronger saturation magnetization is a way to enhance the magnetic force. Using an MRI system able to provide stronger magnetic field gradients could also optimize the magnetic/drag forces ratio.

As the magnetic force is proportional to the gradient, and saturation magnetization, a permendur sphere (diameter of 3.175mm) submitted to a 70mT/m MRI gradient will encounter 5.71 times more magnetic force than the sample hereby tested.

Experiment 2 aimed at getting a first concrete idea of the imaging problems that will have to be solved in order to control the MR-Sub. There is no direct method of tracking the MR-Sub because of the tremendous three-dimensional complexity and important size of the artifacts.

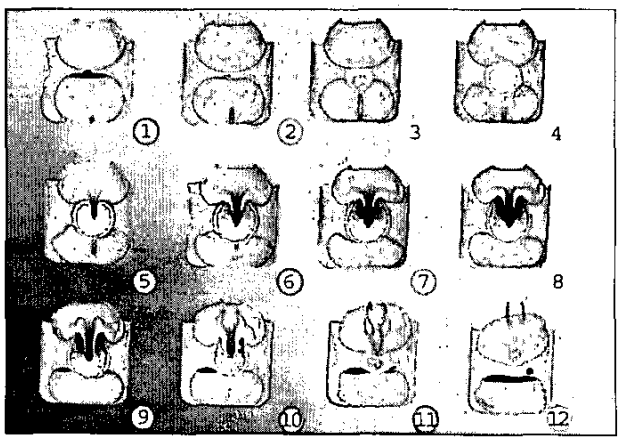

Fig. 5. Imaging series C with slice numbers

Ferromagnetic artefacts arise from the fact that ferromagnetic bodies have a magnetic susceptibility that is several orders of magnitude higher than the one of biological tissues. This behaviour distorts locally the magnetic field of the MRI system and induces imaging problems that are linked to the imaging sequence that is used [12]. MRI images are generated assuming a homogeneous magnetic field; hence they do not take the presence and effect of a ferromagnetic body into account. This presence modifies the Larmor frequency and the relaxation parameters of the hydrogen atoms [9] as well as the positioning gradients [12] and RF pulses. This gives rise to imaging distortions in the intensity and in the position assigned to pixels in the image [13,14].

A ferromagnetic body induces around itself complex three-dimensional distortions of the main magnetic field and of its gradients. The effect of these distortions on the image is even more complex since they affect several steps of the imaging process. Therefore, the link between the ferromagnetic body and the artifact is far from being straightforward.

VI. CONCLUSION

Experiment 1 is the first attempt to control a ferromagnetic body using the magnetic gradients provided by an MRI system. The set-up was fairly simple since its goal was to prove that the concept was viable.

The next steps in these experimentations are to vary flow and gradients altogether in order to achieve one-dimensional real time position control. Then it will be extended to three-dimensional control with tube geometry and tube walls simulating actual vasculature properties.

The MR-Sub project is about controlling a microdevice using an MRI system. It is critical to track this device in real time since failure to do so would have severe repercussions on the health of the patient. An image processing study is currently undertaken in order to bypass the obstacles due to ferromagnetic artifacts. There are two initial approaches that may be investigated. The first one would be to modify the MRI software in order to take into account the presence of the ferromagnetic body at every step of the imaging process. A mathematical model of MR-Sub's magnetization has to be performed [13]. Another approach would be to develop an image-processing algorithm to track a known artifact in the distorted image from its mathematical model or from an artifact database. When the artifact is found, it would be linked to the robot's position.

If image treatment approaches become impractical, the propulsion and tracking tasks may be separated. A ferromagnetic body tracking system may have to be grafted onto the MRI system. Once its position is known, the control of MR-Sub would be potentially feasible.

REFERENCES

[1] T. Morita, M. K. Kurosawa, and T. Higuchi, "Cylindrical shaped micro ultrasonic motor utilizing PZT thin film (1.4 mm in diameter and 5.0 mm long stator transducer)," *Sensors and Actuators, A: Physical: The 10th International Conference on Solid-State Sensors and Actuators TRANSDUCERS '99,Jun 7-Jun 10 1999*, vol. 83, no. 1. May, pp. 225-230, 2000.

[2] R. G. McNeil , R. C. Ritter, B. Wang, M. A. Lawson, G. T. Gillies, K. G. Wika, E. G. Quate, M. A. Howard 3rd, and M. S. Grady, "Functional design features and initial performance characteristics of a magnetic-implant guidance system for stereotactic neurosurgery," *IEEE Trans Biomed Eng*, vol. 42, pp. 793-801, Aug, 1995.

[3] Sendoh, M., Ishiyama, K., Arai, K. I., Jojo, M., Sato, F., and Matsuki, H., "Fabrication of magnetic micro-machine for local hyperthermia," *2002 IEEE International Magnetics Conference (Intermag 2002)*, pp. FU11, Apr. 2002-May 2002.

[4] Rushmer, R. F. *Structure and function of the cardiovascular system*, S. W. B. Saunders Company, 1972.

[5] Milnor, W. R. *Hemodynamics*, Baltimore/London: Williams and Wilkins, 1982.

[6] Jiles, D. *magnetism and magnetic materials*, Chapman and Hall, 1990.

[7] R. M. Wham, O. A. Basaran, and C. H. Byers, "Wall effects on flow past fluid spheres at finite Reynolds number: wake structure and drag correlations," *Chemical Engineering Science*, vol. 52, no. 19. pp. 3345-3367, Oct, 1997.

[8] J.-B. Mathieu, S. Martel, L. Yahia, G. Soulez, and G. Beaudoin, "Preliminary investigation of the feasibility of magnetic propulsion for future microdevices in blood vessels," *BioMedical Materials and Engineering*, unpublished.

[9] Kastler B. *Principes de l'IRM, Manuel d'auto Apprentissage* (In French), Masson, 1994.

[10] White, F. M. *Fluid Mechanics fourth edition*, McGraw and Hill, 1999.

[11] Chen, C.-W. *Magnetism and Metallurgy of Soft Magnetic Materials*, Amsterdam New York Oxford: North-Holland, 1977.

[12] Hendrick R. E. , Russ P. D., and Simon J. H. *MRI: Principles and Artifacts*, Raven Press, 1993.

[13] S. Balac, G. Caloz, G. Cathelineau, B. Chauvel, and J. D. de Certaines, "Integral method for numerical simulation of MRI artifacts induced by metallic implants," *Magnetic Resonance in Medicine*, vol. 45, no. 4, pp. 724-7, Apr, 2001.

[14] Mathieu, J.-B., Martel, S., Yahia, L., Soulez, G., and Beaudoin, G., "Preliminary studies for using magnetic resonance imaging systems as a mean of propulsion for microrobots in blood vessels and evaluation of ferromagnetic artefacts," presented at the Canadian congress on electric and computer engineering, Montreal Canada, 2003.